High Birefringence Liquid Crystal for Fast-Response Phase Modulators †

Qian Yang,[1] Junyu Zou,[1] Haruki Ooishi,[2] Zhuo Yang,[2]
Kifumi Yoshidaya[2] and Shin-Tson Wu[1]
[1]College of Optics and Photonics, University of Central Florida, Orlando, FL
[2]DIC Corporation, Tokyo, Japan

Abstract

We report a high birefringence and low viscosity nematic liquid crystal for phase-only spatial light modulators (SLMs). To achieve 2π phase change at λ = 633 nm with 5 V operation voltage, the measured response time is 2.2 ms at 50°C. Meanwhile, our mixture exhibits no sign of photodegradation for a total dosage of 20 MJ/cm² at a blue laser wavelength λ = 465 nm. Widespread applications of this material for high brightness SLMs, LIDAR, near-eye displays, and head-up displays are foreseeable.

Author Keywords

liquid crystals; liquid-crystal-on-silicon; photostability

1. Introduction

Liquid crystals (LCs) have been widely used in display devices, such as augmented reality (AR) and virtual reality (VR), tablets, computers, TVs, vehicle displays, and data projectors [1–3]. For amplitude modulation, the required phase retardation ($\delta = 2\pi d\Delta n/\lambda$) is about 1π, depending on the LC mode employed [4], where d is the cell gap, Δn is the LC birefringence, and λ is the wavelength. For display applications, the central wavelength is $\lambda \approx 550$ nm and the cell gap is controlled at 3 μm in order to obtain fast response time and high manufacturing yield. Under such conditions, the required Δn is approximately 0.1. For such a low Δn LC material, fluorinated cyclohexane-phenyl compounds [5] are commonly used. These compounds exhibit low viscosity, high resistivity, and excellent photostability.

On the other hand, phase-only liquid-crystal-on-silicon (LCoS) panels have also found widespread application in adaptive optics for wavefront corrections, beam shaping for lithography, telecom as a wavelength selective switch, and multifocal displays for overcoming the vergence-accommodation conflict issue in AR and head-up displays [6]. Recently, LC is combined with metasurfaces to produce high resolution and large deflection angle spatial light modulators (SLMs) for LiDAR-assisted autonomous vehicles [7]. Such an SLM should have 2π phase modulation, less than 3 ms response time, low operation voltage (≤5 V_{rms}, the root-mean-square voltage) without the overdrive and undershoot driving circuitry, and excellent photostability, especially in the blue spectral region.

To achieve fast response time while keeping a low operating voltage, a simple method is to use a thinner cell while keeping 2π phase modulation. LCoS is a reflective device, which means the incident light traverses the LC layer twice. Moreover, the actual operating temperature of an LCoS is 40–50°C due to the thermal effect of CMOS driving circuitries. In the meantime, photostability of the employed high Δn LC materials and alignment layers is essential for extending the SLM lifetime [8].

In this paper, we report a new LC mixture optimized for the LCoS SLMs. Its modest birefringence and low viscoelastic constant jointly contribute to fast response time (~2.2 ms @ 50 °C) and it exhibits an excellent photostability at λ = 465 nm for a dosage over 20 MJ/cm².

2. Material characterization

First, we characterize and compare the physical properties of DIC A4907, Merck TL-216 and UCF-216 [9]. Their phase transition temperatures and physical properties (at T = 22 °C) are summarized in Table 1. We measured the melting temperature (T_m) and clearing temperature (T_c) by differential scanning calorimetry (DSC, TA Instruments Q100). The wide nematic range (-20 °C ~ 80 °C) satisfies the requirement for most LCoS applications. We also measured the dielectric constants with a multifrequency LCR meter, HP-4274. The viscoelastic constant γ_1/K_{11} of each mixture was measured from the free relaxation response time of a test cell. The relatively low γ_1/K_{11} effectively helps to reduce the response time.

Table 1. Measured physical properties of DIC A4970, Merck TL-216 and UCF-216 at T = 22 °C.

LC mixture	A4907	TL-216	UCF-216
T_c (°C)	91.9	80.0	81.8
T_m (°C)	-19	−20	−20
Δn @ 633 nm	0.220	0.205	0.215
$\Delta\varepsilon$ @ 1 kHz	7.3	5.5	7.6
$\varepsilon_\perp$ @ 1 kHz	3.8	4.2	4.2
K_{11} (pN)	13.3	14.4	14.6
K_{33} (pN)	16.3	19.6	---
γ_1/K_{11} (ms/μm²)	12.9	19.0	14.5

2.1. Birefringence

Birefringence determines the cell gap, which in turn affects the response time. To measure Δn, we filled the LC mixture into a homogeneous cell with cell gap d = 5.34 μm. The pretilt angle of the rubbed polyimide alignment layers is about 3°. We sandwiched the cell between crossed polarizers and activated it with a 1 kHz square-wave AC voltage. The sample temperature was controlled by a Linkam heating stage through a temperature programmer TMS94. The birefringence was calculated from the measured phase retardation. Figure 1 depicts the temperature-dependent birefringence at λ = 633 nm (He–Ne laser), where dots represent the measured data and solid lines represent the fitting with following equation:

$$\Delta n = \Delta n_0 S = \Delta n_0 \left(1 - T/T_c\right)^{\beta}. \quad (1)$$

In Equation (1), Δn_0 stands for the extrapolated birefringence at T = 0 K, S is the order parameter, T_c (unit: K) is the clearing temperature of the LC, and exponent β is a material parameter. Both Δn_0 and β can be obtained by fitting the experimental data with Equation (1). Results are listed in Table 2. For convenience, we will use Celsius (°C) instead of Kelvin temperature (K) in the following figures.

 ISSN 0097-996X/21/5203-1416-$1.00

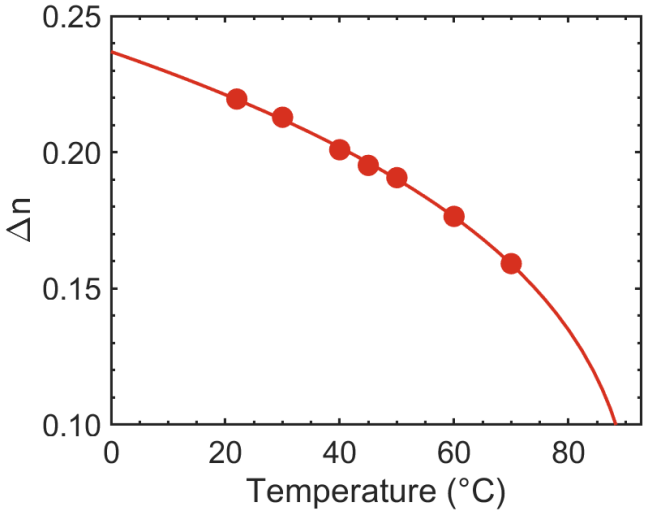

Figure 1. Temperature-dependent birefringence of A4907 at λ = 633 nm and 1 kHz. Dots are measured data and solid lines are fitting curves with Equation (1). The fitting parameters are listed in Table 2.

For a working LCoS device, the operating temperature is about 40-50°C because of the thermal effect from the CMOS backplane and illumination light. Therefore, we measured the wavelength dispersion at 40°C to investigate the electro-optical performances at RGB colors. In experiment, He-Ne laser (λ=632.8 nm) and a tunable Argon ion laser (λ=457 nm, 488 nm, and 514 nm) were used as probing light sources. The obtained results are shown in Figure 2, where dots indicate measured data and solid lines are the theoretical fitting curves with the single-band birefringence dispersion equation:

$$\Delta n = G\frac{\lambda^2\lambda^{*2}}{\lambda^2-\lambda^{*2}}. \qquad (2)$$

In Equation (2), G is a proportionality constant and λ^* is the mean resonance wavelength. Both G and λ^* can be obtained by fitting experimental data with equation (2) and they are listed in Table 2. At λ=633 nm and 40°C, the Δn of A4907 is 0.200.

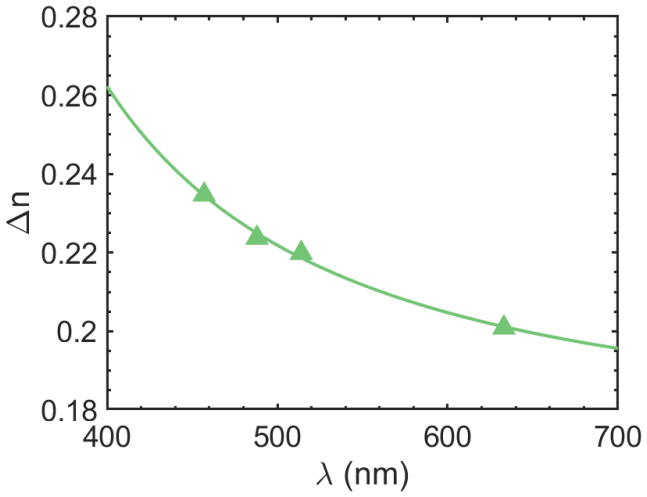

Figure 2. Wavelength dependent birefringence at T=40°C.

2.2. Viscoelastic Constant

We also measured the transient decay time of the LC material and obtained the temperature-dependent viscoelastic constant γ_1/K_{11}, shown by the dots presented in Figure 3. The solid lines represent fittings with following equation:

$$\frac{\gamma_1}{K_{11}} = A\frac{\exp\left(E_a/k_BT\right)}{\left(1-T/T_c\right)^{\beta}}. \qquad (3)$$

In Equation (3), A, E_a, and K_B stand for the proportionality constant, activation energy, and Boltzmann constant, respectively. The fitting parameters are also included in Table 2. From Figure 3 and Equation (3), we can see that γ_1/K_{11} decreases dramatically as the temperature increases and then gradually saturates as the temperature approaches to the clearing point.

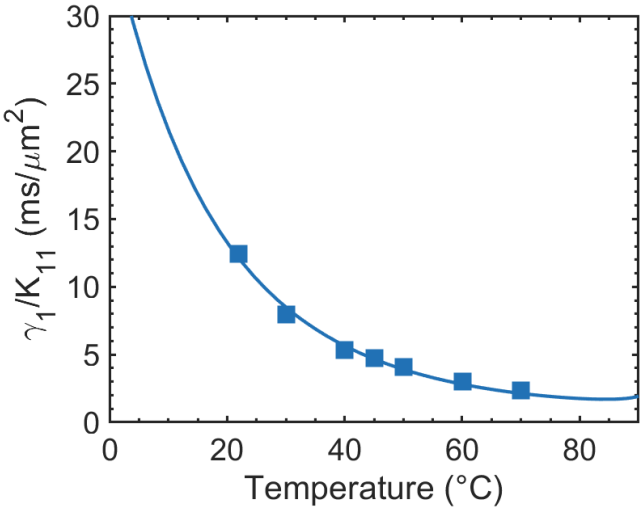

Figure 3. Temperature-dependent viscoelastic constant of DIC A4907. Dots are measured data and solid lines are fitting curves using Equation (3). The fitting parameters are listed in Table 2.

Table 2. Fitting parameters obtained through Equations (1), (2) and (3).

LC mixture	A4907
Δn_0	0.350
β	0.284
G @40°C (μm^{-2})	3.24
λ^*@40°C (μm)	0.232
A (ms/μm^2)	3.11× 10^{-6}
E_a (meV)	274

2.3. Voltage Dependent Phase Change

As mentioned above, for a working LCoS device, its operating temperature is about 40–50 °C due to the thermal effects of CMOS backplane and the high-power light source. Therefore, we focus our studies at two temperatures: 40 °C and 50 °C. The voltage-dependent phase (V-Φ) curves of the material can be converted from the voltage-dependent transmittance (V-T) curve measured at λ = 633nm. Figure 4 (a) and 4(b) depicts the V-Φ curve of DIC A4907 (d = 5.34 μm) at 40 °C and 50 °C, respectively. Although the LCoS is a reflective device, our

measurements were conducted in transmissive cells, because we did not have such a thin LC cell in our labs. Our measured results can be converted to the corresponding reflective cells easily. From Figure 4, the $V_{2\pi}$ of A4907 occurs at 2.6V_{rms} at 40°C and 2.7V_{rms} at 50°C (red lines). To explain the slightly increased $V_{2\pi}$, we should consider two factors as the temperature increases: (1) decreased Δn and (2) decreased threshold voltage (V_{th}). The former is more apparent than the latter, leading to a slightly higher $V_{2\pi}$ at 50 °C. It should be mentioned that our allowed $V_{2\pi}$ is 5 V_{rms}, that means we can use a slightly thinner cell gap to achieve the desired 2π phase change. The *V-Φ* curve of a different cell gap can be extrapolated by simply using the phase retardation equation $\delta = 2\pi d\Delta n/\lambda$. If we operate A4907 at 50 °C, we could use a thinner cell gap (3.95 μm transmissive cell or 1.98 μm reflective LCoS) to obtain $V_{2\pi}$ at 5 V_{rms}, as the blue line shows. A thinner cell gap leads to a faster response time, which will be discussed quantitatively later.

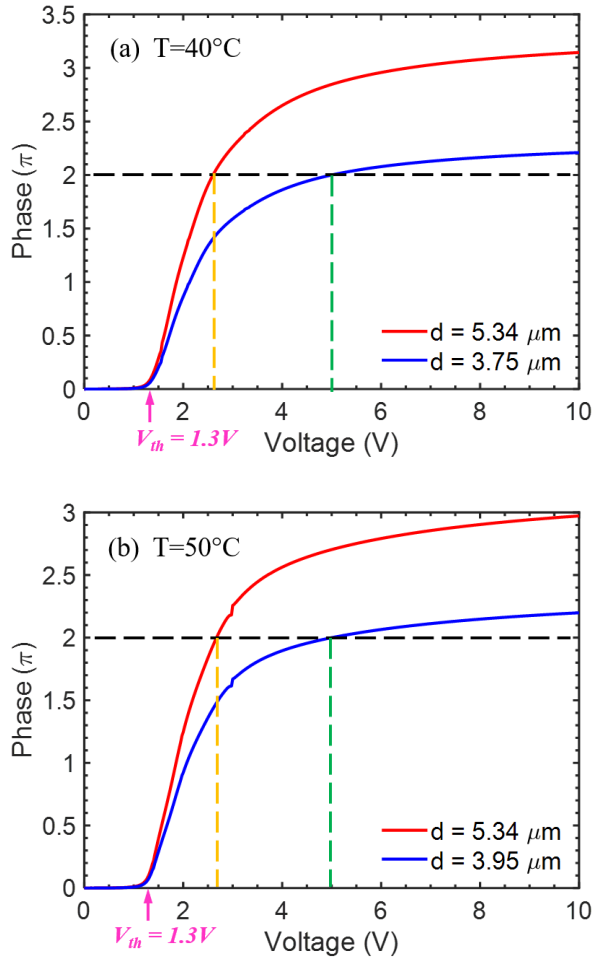

Figure 4. Measured (red line) voltage-dependent phase change of a transmissive A4907 test cell at λ = 633 nm and 1 kHz. Cell gap is d = 5.34 μm, with $V_{2\pi}$ = 2.6 V_{rms} at T = 40 °C in (a) and with $V_{2\pi}$ = 2.7 V_{rms} at T = 50 °C in (b). If we operate A4907 at 50°C, we could use a thinner cell gap (3.95 μm transmissive cell or 1.98 μm reflective LCoS, blue line in (b)) to increase $V_{2\pi}$ to 5 V_{rms}.

2.4. Response Time

The switching time (rise time and decay time) between two gray levels (V_1 and V_2) of an LC phase modulator are governed by the LC cell gap, viscoelastic constant, and operating voltages as:

$$\tau_{on} = \frac{\tau_0}{(V_2 / V_{th})^2 - 1}, \quad (4)$$

$$\tau_{off} = \frac{\tau_0}{\left|(V_1 / V_{th})^2 - 1\right|}, \quad (5)$$

$$\tau_0 = \frac{\gamma_1 d^2}{K_{11}\pi^2}. \quad (6)$$

In Equations (4), (5) and (6), V_{th} is the threshold voltage, V_2 is the high gray-level voltage, V_1 is the low gray-level voltage, and τ_0 is the free relaxation time, i.e., V_1 = 0. From Equations (4) and (5), the response time near V_{th} is sluggish. In Figure 4(b), at 50 °C, because $V_{2\pi}$ of A4907 with cell gap d = 5.34 μm is not too far from the threshold voltage (V_{th} = 1.3 V_{rms}), according to Equation (4) the rise time will be slow. From our previous studies [10], the average gray-to-gray rise time and decay time is about the same as the sum of turn-on time (V_2 = 8th gray level; in our case 5 V) and free relaxation time (V_1 = 0).

Table 3 summarizes the measured response time of A4907, using a d = 5.34 μm test cell at λ = 633 nm and T = 40 °C and 50 °C. From Table 3, A4907 can achieve 8.25 ms at T = 40 °C with $V_{2\pi}$ = 2.6 V_{rms}, and 6.23 ms at 50 °C with $V_{2\pi}$ = 2.7 V_{rms}. It should be mentioned that our allowed $V_{2\pi}$ is 5 V_{rms}. If we operate A4907 at 40 °C, we can use a thinner cell gap (3.75 μm in transmissive mode or 1.88 μm in reflective LCoS @ 40 °C) to increase $V_{2\pi}$ to 5 V_{rms}. Under such condition, the rise time can be reduced. From Table 3, the total response time τ_{on} + τ_{off} = 2.46 ms. If we increase the operation temperature to 50 °C, the response time can be further reduced to 2.20 ms, using a 1.98 μm cell gap in reflective mode, which enables LCoS SLM to operate at > 400 Hz.

Table 3. Measured response time of a transmissive A4907 cell with d = 5.34 μm, and the extrapolated response time to the corresponding reflective cells at 40 °C and 50 °C with λ = 633 nm.

***T* (°C)**	40	**40**	50	**50**
***d* (μm)**	5.34	**3.75**	5.34	**3.95**
***Vth* (V)**	1.3	**1.3**	1.3	**1.3**
***V2π*(V)**	2.6	**5.0**	2.7	**5.0**
***τon* (ms)**	16.63	**1.78**	11.58	**1.49**
***τoff* (ms)**	16.35	**8.06**	13.34	**7.30**
τ_{total} (ms) Transmissive	32.98	**9.85**	24.92	**8.78**
τ_{total} (ms) Reflective	8.25	**2.46**	6.23	**2.20**

3. Photostability

LCoS projection displays are usually illuminated by a relatively high-power arc lamp, light emitting diodes, or lasers. Even if the

ultraviolet and infrared parts of the arc lamp light source are filtered out, the remaining blue light may still degrade the device lifetime. These high-energy photons could decompose the LC compounds or deteriorate the polyimide alignment layer, which in turn changes the pretilt angle of the LC and consequently affects the electro-optic properties. Inorganic SiO_x alignment layers have been found to sustain long-term UV and blue light exposure without damage [11], but the photostability of high Δn LC materials, especially in the blue spectral region, have not been investigated thoroughly.

To investigate the photostability, A4907 is filled in a 9.42 µm test cell, using indium tin oxide (ITO)–glass substrates overcoated with a thin inorganic SiO_x alignment layer and exposed to a high-power CW blue diode laser with λ = 465 nm, whose laser intensity was kept at 72 W/cm^2. The sample is exposed for one day and then took out for 30 minutes to check the birefringence and viscoelastic constant. After the measurements, the sample is put back to the irradiation system for further exposure. The measured results are recorded in Figure 5. As the dosage increased, Δn and γ_1/K_{11} remain basically unchanged in the first 20 MJ/cm^2.

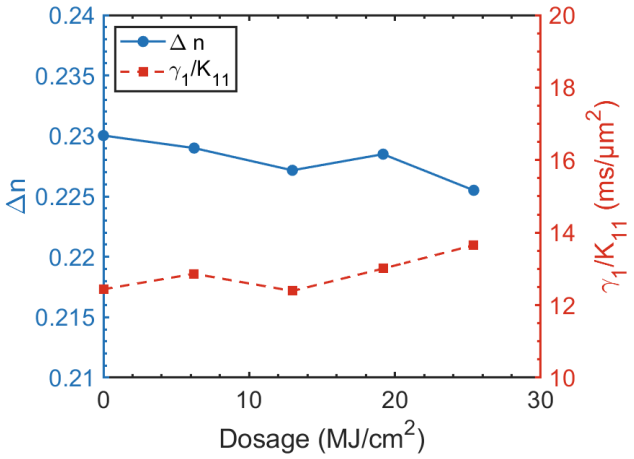

Figure 6. Measured photostability of A4907 with a blue laser at λ = 465 nm at 22 °C. Probing laser λ = 633 nm.

4. Conclusion

In conclusion, we have developed a new LC mixture, designated as A4907, which is suitable for high brightness LCoS SLMs. The mixture exhibits fast response time (~2.20 ms @ 50 °C), low operation voltage (5V_{rms}). DIC A4907 exhibits no sign of photodegradation for a total dosage of 20 MJ/cm^2 at a blue laser wavelength λ = 465 nm. Practical applications of A4907 for laser-based SLMs, LiDAR, high brightness AR displays, and head-up displays are foreseeable.

5. Acknowledgements

The UCF group is indebted to DIC Corporation for providing the LC samples, and Sony Corporation for the financial support.

6. References

1. Schadt M. Milestone in the history of field-effect liquid crystal displays and materials. Japanese Journal of Applied Physics. 2009 Mar 23;48(3S2):03B001.

2. Huang Y, Hsiang EL, Deng MY, Wu ST. Mini-LED, Micro-LED and OLED displays: present status and future perspectives. Light: Science & Applications. 2020 Jun 18;9(1):105.

3. Zhan T, Yin K, Xiong J, He Z, Wu ST. Augmented Reality and Virtual Reality Displays: Perspectives and Challenges. iScience. 2020 Aug 21;23(8):101397.

4. Chen HW, Lee JH, Lin BY, Chen S, Wu ST. Liquid crystal display and organic light-emitting diode display: present status and future perspectives. Light: Science & Applications. 2018 Mar;7(3):17168–17168.

5. Chen HM, Yang JP, Yen HT, Hsu ZN, Huang Y, Wu ST. Pursuing high quality phase-only liquid crystal on silicon (LCoS) devices. Applied Sciences. 2018 Nov;8(11):2323.

6. Zhan T, Xiong J, Zou J, Wu ST. Multifocal displays: review and prospect. PhotoniX. 2020 Mar 30;1(1):10.

7. Li SQ, Xu X, Veetil RM, Valuckas V, Paniagua-Domínguez R, Kuznetsov AI. Phase-only transmissive spatial light modulator based on tunable dielectric metasurface. Science. 2019 Jun 14;364(6445):1087–1090.

8. Yakovenko S, Konovalov V, Brennesholtz M. 6.2: Lifetime of Single Panel LCOS Imagers. SID Symposium Digest of Technical Papers. 2004 May;35(1):64–67.

9. Yang Q, Zou J, Li Y, Wu ST. Fast-response liquid crystal phase modulators with an excellent photostability. Crystals. 2020 Sep;10(9):765.

10. Chen H, Gou F, Wu ST. Submillisecond-response nematic liquid crystals for augmented reality displays. Optical Materials Express. 2017;7(1):195–201.

11. Wen CH, Gauza S, Wu ST. Photostability of liquid crystals and alignment layers. Journal of the Society for Information Display. 2005 Sep;13(9):805-811.